Peculiarities of a Solid-State Synthesis of Multiferroic Polycrystalline $BiFeO_3$

Matjaz Valant,*,† Anna-Karin Axelsson, and Neil Alford

Department of Materials, Imperial College London, Exhibition Road, SW7 2AZ, London, United Kingdom

Received June 29, 2007. Revised Manuscript Received August 23, 2007

Studies of a $BiFeO_3$ synthesis were performed to identify reasons for the appearance of secondary phases, the $Bi_{25}FeO_{39}$- and $Bi_2Fe_4O_9$-type phases, in the reaction product. X-ray diffraction and microstructural analyses, performed on samples with different concentrations of impurities, showed that the impurities in the starting material crucially influence the phase composition of the reaction product. A fraction of the generated secondary phases strongly depends on the nature and concentration of the impurities. The experimental results can be explained by the theoretical consideration of ternary phase relations between Bi_2O_3, Fe_2O_3, and an impurity oxide. Single-phase polycrystalline $BiFeO_3$ was synthesized from ultrapure starting oxides. To avoid using the expensive ultrapure oxides, techniques for reducing the fraction of the secondary phases in the reaction products were developed.

1. Introduction

$BiFeO_3$ is one of the most investigated multiferroic ceramic materials. The paradox, however, is that we still do not understand the basic conditions for a solid-state synthesis of the single phase. Authors repeatedly report problems related to the synthesis of this material, and no direct explanation has been given yet for the persistent appearance of secondary phases.

Problems with the solid-state synthesis of $BiFeO_3$ ceramics were first mentioned by Filipev et al.[1] in 1960. Later, Achenbach[2] reported the same problems. They failed to synthesize single-phase $BiFeO_3$ even by an extensive variation of sintering temperature, time, and atmosphere. Secondary phases in their reaction product were identified to be Bi_2O_3 and $Bi_2Fe_4O_9$. To prepare pure $BiFeO_3$, they synthesized it with an excess of Bi_2O_3, which was afterward removed by leaching in concentrated HNO_3. Later, other authors, who have studied the synthesis of $BiFeO_3$, more precisely defined the chemistry of the secondary phases.[3−5] A more detailed analysis of the Bi_2O_3 secondary phase showed that, in fact, it is sillenite $Bi_{25}FeO_{39}$ that is isostructural to γ-Bi_2O_3. A recent report on the same problem was published by Lufas et al.[6] The authors, whose major expertise is in the field of phase diagrams and solid-state processing, described the problem in the same terms and stressed that the phase fraction of the secondary phases remained constant despite repeated grinding and hundreds of hours of firing at 800 °C.

Parallel to the described efforts, some authors tried to find some indirect methods for the synthesis of pure $BiFeO_3$. Wang et al.[7] reported the synthesis of pure $BiFeO_3$ by a so-called rapid liquid-phase sintering method. They fired a mixture of Bi_2O_3 and Fe_2O_3 at 880 °C for a short time of 450 s with a high heating rate of 100 °C/s. The method was later often used by other authors for the sintering of presumably single-phase $BiFeO_3$.[8] However, the authors have mainly relied on XRD analyses; there are no reports presenting a comprehensive microstructural analysis to confirm the successful synthesis of single-phase $BiFeO_3$. As a part of the present study, we revised this method to gain insight on processes and phase formations related to the rapid liquid-phase sintering method and to perform a detailed microstructural analysis.

Researchers have suggested different reasons for the appearance of the secondary phases. They describe $BiFeO_3$ as being metastable,[9] off-stoichiometric,[5] having a low peritectic decomposition temperature,[10] or that its formation is affected by Bi_2O_3 evaporation.[1,2] All these assumptions are also incorporated in the existing Bi_2O_3−Fe_2O_3 phase diagrams,[9−11] which makes the ambiguities, related to the formation of and phase relations around $BiFeO_3$, even more pronounced.

Crystallographic studies agree on the fact that all crystallographic sites in the $BiFeO_3$ perovskite structure are fully

* Corresponding author. E-mail: matjaz.valant@p-ng.si.
† Current address: University of Nova Gorica, Vipavska 13, 5000 Nova Gorica, Slovenia.

(1) Filipev, V. S.; Smolyaninov, N. P.; Fesenko, E. G.; Belyeav, I. N. *Kristallografiya* **1960**, *5*, 958.
(2) Achenbach, G. D. *J. Am. Ceram. Soc.* **1967**, *50*, 437.
(3) Sosnowska, I.; Peterlin-Neumaier, T.; Steichele, E. *J. Phys. C* **1982**, *15*, 4835.
(4) Fischer, P.; Polomska, M.; Sosnowska, I.; Szymanski, M. *J. Phys. C* **1980**, *13*, 1931.
(5) Morozov, M.; Lomanova, N. A.; Gusarov, V. V. *Russ. J. Gen. Chem.* **2003**, *73*, 1676.
(6) Lufas, M. W.; Vanderah, T. A.; Pazos, I. M.; Levin, I.; Roth, R. S.; Nino, J. C.; Provenzano, V.; Schenck P. K. *J. Solid State Chem.* **2006**, *179*, 3900.
(7) Wang, Y. P.; Zhou, L.; Zhang, M. F.; Chen, X. Y.; Liu, J. M.; Liu, Z. G. *Appl. Phys. Lett.* **2004**, *84*, 1731.
(8) Pradhan, A. K.; Zhang, K.; Hunter, D.; Dadson, J. B.; Loiutts, G. B.; Bhattacharya, P.; Katiyar, R.; Zhang, J.; Sellmyer, D. J.; Roy, U. N.; Cui, Y.; Burger, A. *J. Appl. Phys.* **2005**, *97*, 93903.
(9) Levin, E. M.; Roth, R. S. *J. Res. Natl. Bur. Stand. (U.S.)* **1964**, *68*, 197.
(10) Koizumi, H.; Niizeki, N.; Ikeda T. *Jpn. J. Appl. Phys.* **1964**, *3*, 495.
(11) Speranskaya, E. I.; Skorikov, V. M.; Rode, Y. E.; Terekhova, V. A. *Bull. Acad. Sci. USSR, Div. Chem. Sci. (Engl. Transl.)* **1965**, *5*, 873.

10.1021/cm071730+ CCC: $37.00
Published on Web 10/05/2007

occupied.[12−15] No evidence of a significant cation deficiency has been reported, whereas only a very low (<1%) oxygen deficiency has been assumed from conductivity measurements.[16,17]

In the present work, we studied the solid-state formation of $BiFeO_3$ and the resulting microstructures to provide the proper reasons for the observed problems. We present techniques for minimizing the concentration of the secondary phases and conditions for the synthesis of pure single-phase $BiFeO_3$. We also carefully analyzed the rapid liquid-phase sintering method and explain the results in terms of phase relations.

2. Experimental Procedures

The syntheses of $BiFeO_3$ were conducted using a solid-state reaction technique starting from Bi_2O_3 (Aldrich, 99.9% and Alfa Aesar, 99.9995%) and Fe_2O_3 (BDH, +99% and Alfa Aesar, 99.9995%) powders with a sub-micrometer particle size and different purity. For some experiments, small amounts (0.1 and 0.5 wt %) of impurity oxides, such as SiO_2 (Aldrich, fumed, 99.8%), TiO_2 (Pi-Kem Ltd., 99.9%), and Al_2O_3 (Mandoval Ltd., 99.9%), were deliberately added at this stage. These oxides were added in the form of fine powders (<200 nm). Stoichiometric mixtures of oxides were homogenized in agate mortar and reacted at 800 °C for 5 h. The mixture was weighed before and after heat treatment to determine possible Bi_2O_3 loss due to evaporation. In all cases, the weight difference was negligible (<0.01%). For sintering, the reacted powders were milled in an YSZ planetary mill with YSZ milling balls in acetone medium for 30 min at 250 rpm. The powders were then uniaxially pressed in steel dies into pellets at approximately 150 MPa and sintered at 880 °C for 2−5 h.

The reaction products were analyzed by powder X-ray diffraction (Philips X'pert Pro) using Cu Kα radiation, an X'Celerator detector (Philips Analytical) equipped with a diffracted beam monochromator. Polished ceramic samples were thermally etched for microstructural analysis at 750 °C for 15 min and were gold-coated. Microstructural and energy dispersive X-ray (EDX) analyses of the ceramics were conducted using a JEOL 840A scanning electron microscope and INCA 4.07 (Oxford Instruments) software.

3. Results and Discussion

Initial $BiFeO_3$ samples, analyzed within this study, were prepared by a regular solid-state method, which has been typically used by other authors. A detailed XRD analysis confirmed the previous observations and showed the presence of a small fraction of a sillenite phase (Figure 1). Even a detailed, high-resolution XRD scan did not show the presence of any other secondary phase. However, microstructural and EDX analyses of the sintered samples showed the presence of two secondary phases. They were identified to be sillenite $Bi_{25}FeO_{39}$ and $Bi_2Fe_4O_9$. The reason why the XRD detection limit for $Bi_2Fe_4O_9$ is so low in such phase assemblages is due to the considerable difference in the atomic scattering factors. The very heavy Bi^{3+} ion with its 80 electrons scatters X-rays much more efficiently than the much lighter Fe^{2+} and O^{2-} with 24 and 10 electrons, respectively. The concentration of the heavy Bi ions is much lower in $Bi_2Fe_4O_9$ then in $Bi_{25}FeO_{39}$; therefore, it is reasonable to expect that the detection limit for $Bi_2Fe_4O_9$ will be much lower.

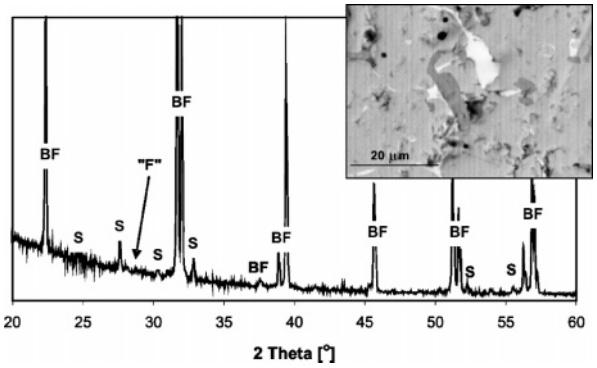

Figure 1. XRD pattern of Bi_2O_3−Fe_2O_3 mixture reacted at 800 °C for 5 h in air and a backscattered electron image of the sample sintered at 880 °C for 5 h. The gray, white, and dark phases are $BiFeO_3$ (BF), $Bi_{25}FeO_{39}$ (S), and $Bi_2Fe_4O_9$ (F). The arrow shows the position of the most intensive $Bi_2Fe_4O_9$ diffraction line (121).

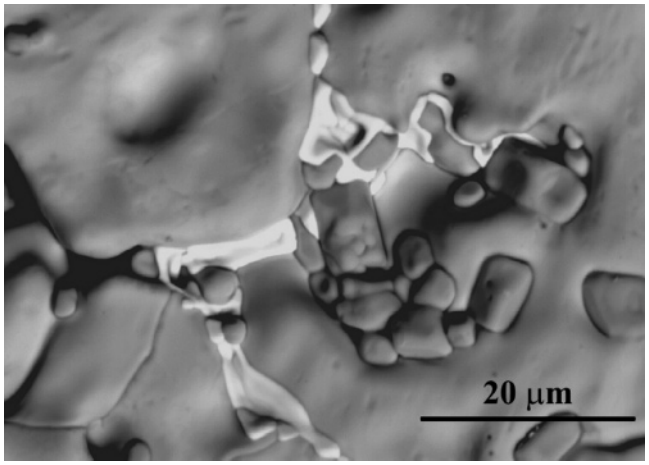

Figure 2. Backscattered electron image of thermally etched $BiFeO_3$ ceramics sintered at 880 °C for 5 h. The image shows the grain-boundary sillenite phase in contact with the matrix $BiFeO_3$ phase and the small $Bi_2Fe_4O_9$ grains.

In this work, we assumed that analyzed samples were in their equilibrium state. Several experimental observations support such an assumption. A repeated firing and grinding did not change the initially observed phase composition and phase fractions. The same has been reported by many other authors.[2,6] In addition, a detailed inspection of the microstructures showed that it is a common feature that $Bi_{25}FeO_{39}$ and $Bi_2Fe_4O_9$ grains share an interface (−i.e., are in a physical contact (Figure 2)). According to all versions of published binary phase diagrams,[10,11] these phases are not thermodynamically compatible and should, at an elevated temperature, react to form $BiFeO_3$.

If our assumption is correct, then we can explain the equilibrium existence of the three phases only by the fact that the system did, during the processing, cease from being binary. To satisfy the Gibbs' phase rule, at least one another

(12) Moreau, J. M.; Michel, C.; Gerson, R.; James, W. J. *J. Phys. Chem. Solids* **1971**, *32*, 1315.
(13) Tutov, A. G. *Solid State Phys.* **1969**, *11*, 2681.
(14) Kubel, F.; Schmid, H. *Acta Crystallogr., Sect. B: Struct. Sci.* **1990**, *46*, 698.
(15) Sosnowska, I.; Schäfer, W.; Kockelmann, W.; Andersen, K. H.; Troyanchuk, I. O. *Appl. Phys. A: Mater. Sci. Process.* **2002**, *74*, 1040.
(16) Yuan, G. L.; Or, S. W.; Wang, Y. P.; Liu, Z. G.; Liu, J. M. *Solid State Commun.* **2006**, *138*, 76.
(17) Li, M.; MacManus-Driscoll, J. L. *Appl. Phys. Lett.* **2005**, *87*, 252510.

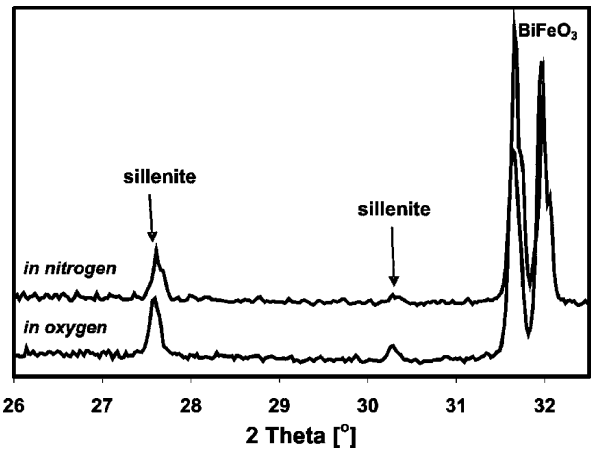

Figure 3. XRD pattern of $Bi_2O_3-Fe_2O_3$ mixture reacted at 800 °C for 5 h in an oxygen and nitrogen atmosphere.

component (besides Bi_2O_3 and Fe_2O_3) should be introduced to explain this three-phase system. The additional components are reduced Fe species or impurities.

We performed a very straightforward test to determine the possible influence of the reduced Fe species on the phase composition of the reaction product. Two batches of a same 1:1 mixture of Bi_2O_3 and Fe_2O_3 were synthesized under the same conditions in the same furnace. One batch was synthesized in oxygen while another batch was synthesized in a nitrogen atmosphere. If the presence of Fe^{2+} is the reason for the appearance of the secondary phases, then in the nitrogen atmosphere, where a much higher concentration of Fe^{2+} is expected, the fraction of the secondary phases must significantly increase as compared to the oxygen atmosphere. An XRD analysis of these prepared powders showed negligible differences in phase composition with no significant change in the fraction of the secondary phases (Figure 3). Hence, we excluded this possibility from further study.

3.1. Influence of Impurities. An impurity ion can interact with the system in four different ways. It can incorporate into a crystal structure of (i) $BiFeO_3$, (ii) sillenite, (iii) $Bi_2Fe_4O_9$, or (iv) does not interact with these phases. Two of these scenarios would not generate a significant fraction of secondary phases. It is straightforward that if an impurity ion incorporates into the $BiFeO_3$ matrix phase, a small amount of Bi or Fe is in excess and forms a small amount of either sillenite or $Bi_2Fe_4O_9$. A simple stoichiometric calculation shows that for a reasonable purity of starting Bi_2O_3 and Fe_2O_3 powders (e.g., 99.9%), the fraction of the secondary phases would not exceed 0.5 vol %, which is much lower than the XRD detection limit. In the case when impurity ions do not interact with the present phases, they remain on the grain boundaries and do not cause detectable changes in the phase composition.

When an impurity ion incorporates into the sillenite crystal structure, a partial or a complete sillenite solid solubility range can be expected in the corresponding ternary phase diagram (Figure 4). Regardless of the extension of the sillenite solid solubility limit, every departure from the binary conditions will necessarily result in the formation of three phases: $BiFeO_3$, $Bi_2Fe_4O_9$, and the sillenite phase. Because of the special position of these phases in the phase diagram, the phase fields are extremely elongated, and small changes

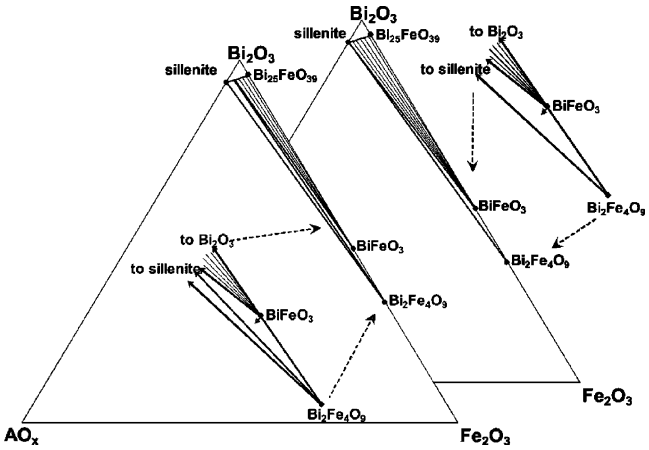

Figure 4. Relevant phase relations in a ternary phase diagram of Bi_2O_3, Fe_2O_3, and an impurity oxide. The diagram shows the case when the impurity oxide forms a sillenite with a partial or complete solid-solubility range with $Bi_{25}FeO_{39}$. The gray arrows in the enlarged portions show the shift of a nominal composition due to the presence of an impurity oxide.

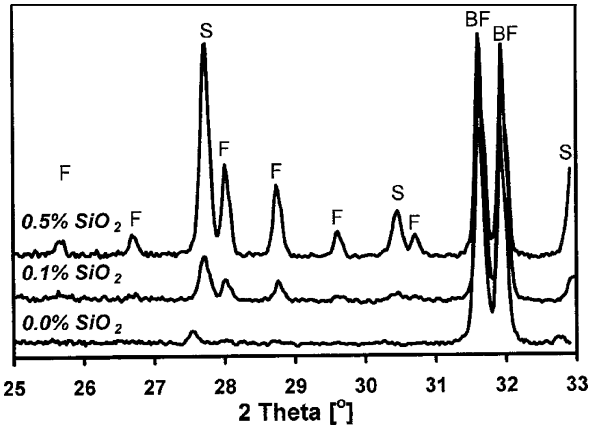

Figure 5. XRD pattern of $Bi_2O_3-Fe_2O_3$ mixture with addition of 0.1 and 0.5% SiO_2 reacted at 800 °C for 5 h in air (S: $Bi_{12}SiO_{20}$; F: $Bi_2Fe_4O_9$; and BF: $BiFeO_3$).

in a nominal composition are expected to give large changes in an equilibrium phase composition. A fraction of the phases can be calculated from given stoichiometric relationships as a function of a solid solubility limit, the concentration of the impurities, and the valence state of the impurity ion. For any combination of the parameters, the calculations showed that only a small amount of impurities generates a high fraction of the secondary phases. For example, 0.1 mol % impurities with a 4+ charge (i.e., A^{4+} ion) and a full sillenite solubility range would generate a 3.1 vol % sillenite phase with the formula $Bi_{12}AO_{20}$ and 7.3 vol % $Bi_2Fe_4O_9$. These are concentrations that are easily detected by XRD analysis. In the case that the sillenite solubility range is narrower, the fraction of the secondary phases would progressively increase. The calculation for 0.5 mol % impurities shows even further degradation of $BiFeO_3$. Only the 57.8 vol % $BiFeO_3$ phase remains in such a sample together with the 12.6 vol % sillenite $Bi_{12}AO_{20}$ and 29.5 vol % $Bi_2Fe_4O_9$.

To confirm the calculations experimentally, we deliberately added small amounts of impurities into a mixture of Bi_2O_3 and Fe_2O_3. In Figure 5, it can be seen that the addition of 0.1 and 0.5 wt % SiO_2 dramatically changed the phase composition after firing. The observed changes followed the calculated predictions qualitatively as well as quantitatively.

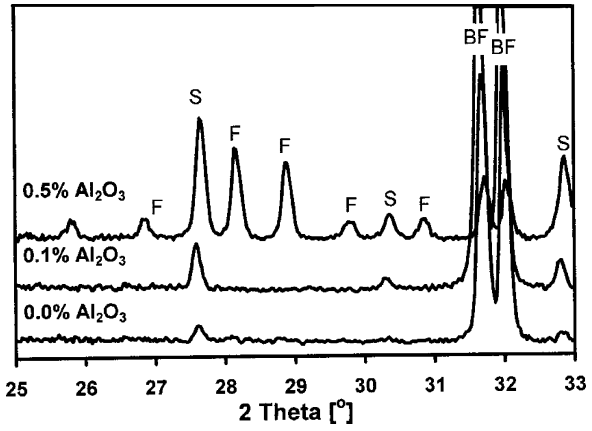

Figure 6. XRD pattern of $Bi_2O_3-Fe_2O_3$ mixture with addition of 0.1 and 0.5 wt % Al_2O_3 reacted at 800 °C for 5 h in air (S: $Bi_{25}FeO_{39}$; F: $Bi_2Fe_{4-x}Al_xO_9$; and BF: $BiFeO_3$).

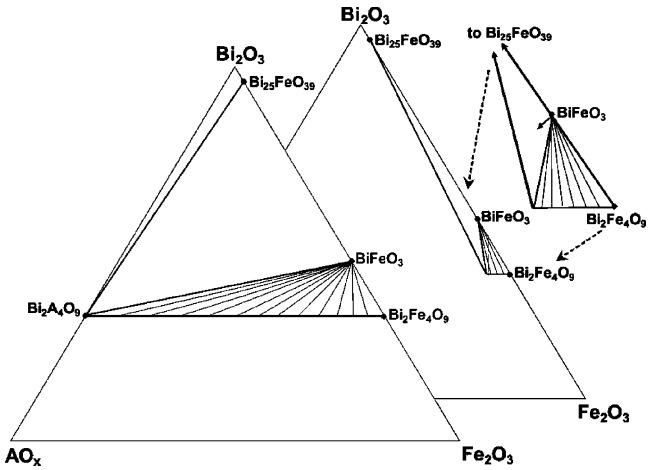

Figure 7. Relevant phase relations in a ternary phase diagram of Bi_2O_3, Fe_2O_3, and an impurity oxide. The diagram shows the case when the impurity oxide can partially or a completely substitute Fe^{3+} in $Bi_{25}FeO_{39}$. The gray arrows in the enlarged portion show the shift of a nominal composition due to the presence of an impurity oxide.

Increasingly higher fractions of sillenite and $Bi_2Fe_4O_9$ were determined with the increase in the concentration of the impurity ion from 0.1 to 0.5 wt %. In addition, the positions of the sillenite diffraction lines corresponded to $Bi_{12}SiO_{20}$ and not to $Bi_{25}FeO_{39}$, which confirmed the phase relations from Figure 4.

Impurity ions can also incorporate into the $Bi_2Fe_4O_9$ phase. An example of such an impurity is Al_2O_3. As can be seen from Figure 6, the addition of 0.1 and 0.5 wt % Al_2O_3 resulted in the formation of a large amount of secondary phases. XRD and microstructural analyses showed the presence of $Bi_{25}FeO_{39}$, $BiFeO_3$, and Al-containing $Bi_2Fe_4O_9$. The concentration of Al in $Bi_2Fe_4O_9$ was determined by elemental EDX microanalysis to be $Bi_2(Fe_{3.7}Al_{0.3})O_9$. The stoichiometric calculations showed that a fraction of the secondary phase is to a great extent influenced by the position of the $Bi_{25}FeO_{39}-Bi_2Fe_4O_9$ (ss) tie line (Figures 7 and 8). When the solid solubility range is large, the phase field between $BiFeO_3$, $Bi_{25}FeO_{39}$, and $Bi_2Fe_4O_{9(ss)}$ is vast, and the impurities have no detectable influence on the phase composition. However, when the solid solubility is low, the phase field in the corresponding phase diagram becomes very stretched out, and the presence of small amounts of impurities

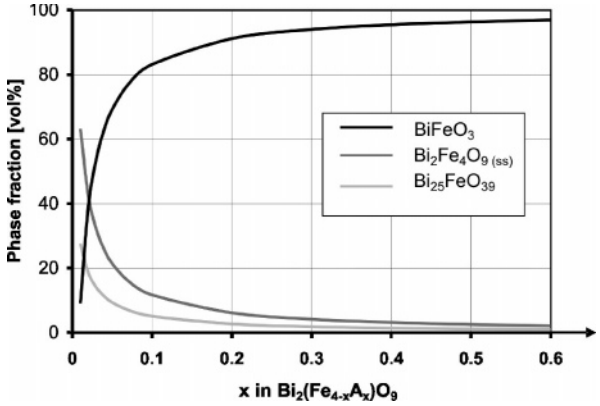

Figure 8. Stoichiometric calculations of the phase composition vs homogeneity range of $Bi_2Fe_{4-x}A_xO_9$ for the presence of 0.1 mol% impurity oxide (according to the phase relations in Figure 7).

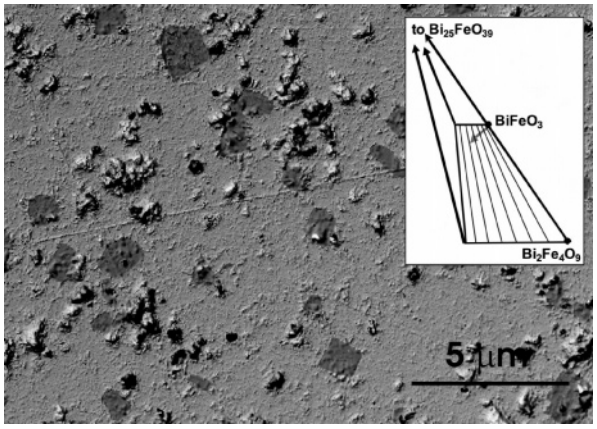

Figure 9. Backscattered electron image of $BiFeO_3$ ceramics with the addition of 0.5% TiO_2 sintered at 880 °C for 5 h in air (dark phase: $Bi_2Fe_4O_9$ and matrix phase: $BiFeO_3$). The inset schematically shows the relevant phase relations in the $Bi_2O_3-Fe_2O_3-TiO_2$ phase diagram.

will again cause an extensive change in the phase composition of the reaction product (see Figure 7). Stoichiometric calculations show that for $Bi_2Fe_{4-x}A_xO_9$ with $x_{lim}= 4$ (complete solid solubility), the presence of 0.1 and 0.5 mol % impurities generates <0.5 and 2.3 vol % secondary phases, respectively. When $x_{lim} = 0.3$, as in the case of Al_2O_3, the fraction of the secondary phases increases to 6 vol %. An increase in the impurity concentration to 0.5 mol % at such conditions causes the formation of 26 vol % secondary phases.

Another impurity, tested within our study, is TiO_2. In contrast to Si^{4+} and Al^{3+}, the ionic radius of Ti^{4+} is similar to Fe^{3+} (0.605 and 0.55 Å for CN = 6),[18] and partial substitution on the perovskite B-site can be expected. Because an aliovalent substitution requires charge compensation, the solid solubility range is usually small. Nevertheless, for the $Bi_2O_3-Fe_2O_3$ system, the existence of even a small solid solubility range has a profound influence on the phase relations. Our experimental results showed that the ceramics with TiO_2 as an impurity exhibit only two phases: $BiFeO_3$ and $Bi_2Fe_4O_9$, both containing small amounts of Ti (Figure 9). The microanalysis showed that approximately 0.5 and 1 mol % Ti was incorporated in $BiFeO_3$ and $Bi_2Fe_4O_9$,

(18) Shannon, R. D. *Acta Crystallogr., Sect. A: Found. Crystallogr.* **1976**, *32*, 751.

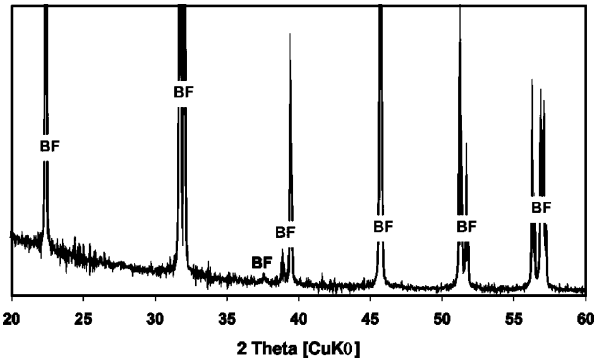

Figure 10. XRD pattern of single-phase $BiFeO_3$ prepared from ultrapure Bi_2O_3 and Fe_2O_3 (99.9995%). The mixture was reacted at 800 °C for 5 h in air.

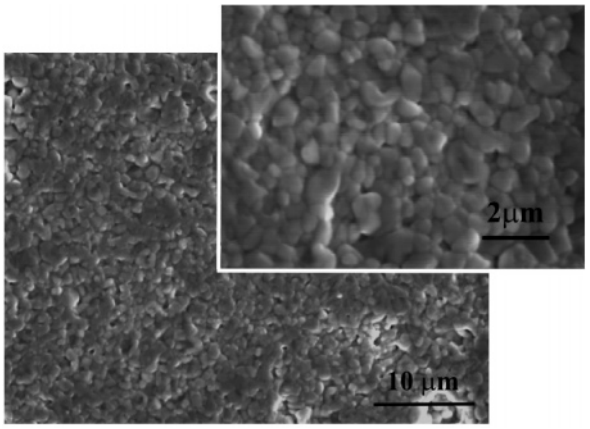

Figure 11. SEM image of $BiFeO_3$ ceramics prepared from ultrapure Bi_2O_3 and Fe_2O_3 (99.9995%). The ceramics was sintered at 880 °C for 5 h in air.

respectively. No sillenite phase was detected in these samples. The observed phase composition corresponds to the situation in the corresponding phase diagram. The inset in Figure 9 shows the shift in the nominal composition, which results from the presence of TiO_2 impurities. The nominal composition moves into a two-phase region between two solid solutions, both identified in our study.

3.2. Synthesis of Single-Phase $BiFeO_3$ Ceramics. The key experiment to confirm that impurities are the reason for the observed problems with the synthesis of $BiFeO_3$ is the synthesis of single-phase polycrystalline $BiFeO_3$ using ultrapure starting oxides. We undertake this experiment using 99.9995% pure Bi_2O_3 and Fe_2O_3. Special care was taken to prevent contamination of the powders during the processing. Only steel, YSZ, and Pt laboratory equipment were used. During the heat treatment, the green pellets were buried in a sacrificial powder. The XRD pattern of the synthesized powder is shown in Figure 10. Only diffraction lines of $BiFeO_3$ are present in the XRD pattern, while even a high-resolution scan did not reveal any presence of secondary phases. The powder was also pressed into a disc and sintered at 880 °C for 5 h. Microstructural analysis confirmed the single-phase composition of the ceramics (Figure 11). In contrast to the samples containing the sillenite phase, the grains remained small (sub-micrometer size). The sillenite phase melts at the sintering temperature and causes the extensive grain growth. In the case of ultrapure $BiFeO_3$ ceramics, no liquid phase was present during the sintering; hence, the grains remained small.

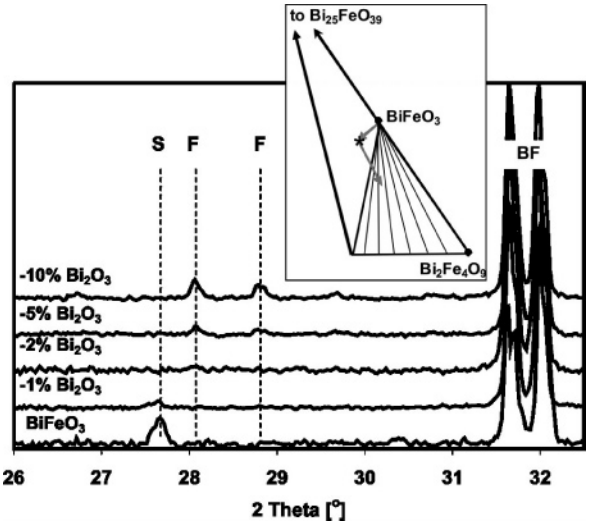

Figure 12. XRD patterns of $Bi_2O_3-Fe_2O_3$ mixture with deficiency of Bi_2O_3, reacted at 800 °C for 5 h in air (S: $Bi_{25}FeO_{39}$; F: $Bi_2Fe_4O_{9(ss)}$: and BF: $BiFeO_3$). The inset shows detail from a quasi-ternary phase diagram of Bi_2O_3, Fe_2O_3, and an impurity oxide. The gray arrows show a shift of a nominal composition due to the presence of inherent impurities and Bi_2O_3 deficiency, respectively.

3.3. Rapid Liquid-Phase Sintering. Some authors have reported that by using a so-called rapid liquid-phase sintering method, single-phase $BiFeO_3$ can be synthesized.[7,16] As they have not reported on formation mechanisms and performed any detailed phase analysis (apart from XRD analyses), we revised this method in light of the described phase relations.

We exactly repeated the experimental procedure reported by Yuan et al.[16] The mixture of powders (99.9% grade) with a <1 μm average particle size was rapidly heated to 855 °C (by insertion into a preheated furnace), dwelled for 5 min, and rapidly cooled to room temperature. XRD analysis confirmed the results described by the authors:[16] the diffraction lines of the secondary phases were not present. During this experiment, the mass loss was monitored by weighing the mass of the dried powder before and after heat treatment. A mass loss of 0.7% was detected, which can be ascribed to the volatilization of Bi_2O_3. The melting points of Bi_2O_3 and $Bi_{25}FeO_{39}$ (825 and 785 °C, respectively)[11] are lower than the firing temperature. During this rapid firing process, Bi_2O_3 and $Bi_{25}FeO_{39}$ melt before they manage to react completely with Fe_2O_3 to form $BiFeO_3$; hence, the method is called rapid liquid-phase sintering. The melting increases the Bi_2O_3 partial pressure and Bi_2O_3 volatilization. Microstructural analysis did not show the presence of the sillenite phase, whereas the $Bi_2Fe_4O_9$ phase was still present.

We simulated this process by preparing mixtures with a controlled deficiency of Bi_2O_3 and fired them at regular conditions, described in the Experimental Procedures, for which no Bi_2O_3 loss occurred. The results in Figure 12 show exactly the same trend as was seen for the rapid liquid-phase sintering. With the increased Bi_2O_3 deficiency, a fraction of the sillenite phase decreased. A reason for the decrease can be deduced from the phase diagram (see the inset in Figure 12). With the decrease in the Bi_2O_3 content, the nominal composition moves from a ternary $Bi_{25}FeO_{39}-BiFeO_3-Bi_2Fe_4O_{9(ss)}$ phase field into the binary $BiFeO_3-Bi_2Fe_4O_{9(ss)}$ phase field. As the scattering factors for $Bi_2Fe_4O_{9(ss)}$ are rather

low as compared to $BiFeO_3$, the diffraction lines do not appear in the XRD pattern, and the synthesis appears to give a single-phase product. With a further Bi_2O_3 deficiency, the fraction of $Bi_2Fe_4O_{9(ss)}$ increases more, and the phase appears in the XRD pattern.

Conclusion

Our studies on the synthesis of single-phase polycrystalline $BiFeO_3$ showed that the successful synthesis of single-phase powder essentially depends on the purity of the starting materials. The impurities force the $Bi_2O_3-Fe_2O_3$ system to shift to a quasi-ternary system and the nominal composition to move into a phase field with a sillenite phase, such as $Bi_{25}FeO_{39}$. As a result of the formation of the sillenite phase with a high concentration of Bi^{3+} ions, the fraction of the other secondary phase, $Bi_2Fe_4O_9$, increases. As a final consequence, a small concentration of impurities generates a large fraction of secondary phases. Single-phase polycrystalline $BiFeO_3$ was synthesized from ultrapure starting oxides. To avoid using expensive ultrapure oxides, the amount of the secondary phases can be reduced by a small Bi_2O_3 deficiency. This effectively occurs in the rapid liquid-phase sintering method.

CM071730+